The Microfiber Loop Resonator: Theory, Experiment, and Application

M. Sumetsky, Y. Dulashko, J. M. Fini, A. Hale, and D. J. DiGiovanni

***Abstract*—This paper describes the theory of a microfiber loop resonator (MLR) and experimentally demonstrates a high quality factor MLR in free space. The MLR is fabricated from the $\sim$ 1-μm diameter waist of a biconical fiber taper using the CO_2 laser indirect heating technique. The high coupling efficiency of an MLR is achieved through an adiabatically slow variation of the microfiber diameter in the coupling region. An MLR-loaded Q-factor of 120 000 and an intrinsic Q-factor of 630 000 were demonstrated. As an application, the performance of an MLR as an ultrafast direct contact temperature sensor is also demonstrated. The MLR heating/cooling relaxation time was measured to be $\sim$ 3 μs, in good agreement with the developed theory.**

***Index Terms*—Microfibers, optical fiber coupling, optical fibers, optical resonators, ring resonators.**

I. Introduction

THERE has been growing interest in developing fabrication methods and applications of low-loss optical microfibers, which are fabricated by drawing conventional silica optical fibers to diameters in the order of a micrometer [1]–[7]. The prospective advantages of microfiber devices compared to lithographic photonic circuits are their much smaller internal and connection losses, compactness, and potential for new functionalities. In fact, the propagation losses of silica microfibers with diameters close to a micrometer were measured to be $\sim 10^{-3}$ dB/mm [3], which is an order of magnitude less than the lowest losses reported for planar photonic waveguides fabricated lithographically [8]. Prospectively, the transmission losses of silica microfibers could be as small as those in single-mode optical fibers and in silica microcavities [4], i.e., $\sim 10^{-7}$ dB/mm. In addition to their small losses, optical microfibers are attractive because of the feasibility of new three-dimensional (3-D) microdevices, which can be composed of microfibers but cannot be realized with other technologies. An example is a self-coupling microfiber coil, which can be fabricated by wrapping the microfiber around an optical rod [5]. Due to its 3-D vertical arrangement, a microfiber coil can be dramatically smaller than planar lithographic photonic circuits with similar functionalities. In some cases, the transmission spectrum of the microfiber coil can be qualitatively different from that of a similar planar photonic circuit composed of rings [9]. The microfiber device can be fabricated of the waist of a biconical fiber taper, which, thereby, performs the low-loss input and output connections. Thus, the problem of connection losses, which is significant for planar photonic circuits, can be naturally solved in microfiber circuits.

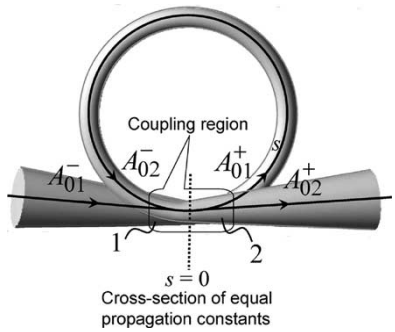

Fig. 1. Illustration of an MLR. The coupling region is outlined. The numbers 1 and 2 correspond to the coupled microfiber segments 1 and 2.

The microfiber loop resonator (MLR) illustrated in Fig. 1 is the simplest microfiber coil resonator (MCR) with a single turn. This device is a miniature version of a fiber loop resonator, which was created for the first time back in 1982 from a conventional single-mode fiber and a directional coupler [10]. Later, Caspar and Bachus [11] demonstrated a 2-mm diameter MLR fabricated of a 8.5-μm diameter waist of an optical fiber taper. The diameter of the microfiber was too large to ensure sufficient interfiber coupling. In order to enhance the coupling efficiency, the MLR was imbedded into a silicone rubber having a refractive index close to the index of the microfiber. At wavelengths of ~ 1.5 μm, the Q-factor of the MLR fabricated in [11] was Q $\sim$ 27 000. Recently, in [1], [6], and [7], microloops fabricated of a micrometer-order diameter microfiber were investigated. A microloop with microfiber diameter of 0.95 μm was demonstrated in [1]. The preliminary measured value of its Q-factor at a wavelength of ~ 1.5 μm was $\sim$ 1500. In [6], a microloop fabricated of a 0.7-μm diameter microfiber exhibited strong periodic interferometric transmission power spectral oscillations with extinction ratio $\sim$ 18 dB at wavelengths of 1.5 μm. In [7], the MLR fabricated of a 0.66-μm diameter microfiber had a Q-factor of $\sim$ 15 000 and, in the regime of critical coupling, exhibited transmission spectral oscillations with an extinction ratio of $\sim$ 34 dB. In this paper, we report our recent results on further increasing the Q-factor of the MLR and its application as an ultrafast direct contact temperature sensor. The abbreviated results were published in our OFC 2005 postdeadline paper [12]. In Section II, the theory of the MLR is discussed. We present the general expression for the transmission amplitude for lossless and polarization-independent MLR. This expression takes into account the roundtrip losses with a complex-valued propagation constant. We discuss the

Manuscript received July 20, 2005; revised October 5, 2005.

The authors are with the OFS Laboratories, Somerset, NJ 08873 USA (e-mail: sumetski@ofsoptics.com).

Digital Object Identifier 10.1109/JLT.2005.861127

dependence of the MLR Q-factor on the propagation losses and coupling efficiency and consider, in particular, the case of a microfiber having a slowly varying radius. In Section III, we describe the method for drawing the microfibers using the CO_2 laser indirect heating technique and the method of creating an MLR in free space. The fabricated MLRs exhibit amazingly smooth and uniform spectral characteristics in the full C-band, demonstrating a loaded Q-factor of up to 120 000 and an intrinsic Q-factor of up to 630 000. In Section IV, we consider the theory of microfiber heating and cooling using the lumped system equation. For a microfiber with a diameter ~ 1 μm, we estimate the charact eristic temperature relaxation time to be ~ 2 μs. Next, we experimentally demonstrate an MLR resonator subjected to periodic ON/OFF heating with the CO_2 laser beam. The measured cooling and heating time was ~ 3 μs, in good agreement with the theoretically predicted value. Section V discusses and summarizes the results of this paper.

II. Theory of an MLR

A. Basic Equations

The theory of the MLR, illustrated in Fig. 1, can be developed by combining the theory of ring resonators [10], [13]–[15] and the theory of directional couplers [16]–[18]. It is assumed below that the MLR is comprised of a single-mode fiber. For simplicity, we ignore coupling between polarization states, referring the reader to [16], [18], and references therein for the theory of polarization mode couplers. Away from the coupling region, for each of the polarizations, the electric field component of the electromagnetic field propagating along the microfiber has the form

$$\mathbf{E}^{(0)}(\mathbf{r}) = \exp\left(i\int^{s}\beta(s)\,ds\right)\mathbf{F}(\mathbf{r}) \tag{1}$$

where $\beta(s)$ is the propagation constant, which can slowly vary along the microfiber length s, and the vector function $\mathbf{F}(\mathbf{r})$ is the local transverse mode corresponding to the propagation constant $\beta(s)$. The propagation constant and the transverse mode are found from the solution of the transverse wave equation [16] having the coordinate s as a parameter. Functions $\beta(s)$ and $\mathbf{F}(\mathbf{r})$ are, generally, polarization dependent. Equation (1) assumes that the transverse mode $\mathbf{F}(\mathbf{r})$ is a slow function of s compared to the exponential $\exp(i\int^{s}\beta(s)\,ds)$. In the approximation of the coupling wave equations, the electromagnetic field in the coupling region is expressed as a linear combination of solutions given by (1) in microfiber segments 1 and 2 (Fig. 1), i.e.,

$$\mathbf{E}(\mathbf{r}) = \left(A_1(s)\mathbf{F}_1(\mathbf{r}) + A_2(s)\mathbf{F}_2(\mathbf{r})\right)\exp\left(i\int_0^{s}\beta(s)\,ds\right)$$

$$\beta(s) = \frac{1}{2}\left(\beta_1(s)+\beta_2(s)\right) \tag{2}$$

where $\beta_1(s)$ and $\beta_2(s)$ are the propagation constants and $\mathbf{F}_1(\mathbf{r})$ and $\mathbf{F}_2(\mathbf{r})$ are the transverse modes in segments 1 and 2, respectively. We define the lower limit of integration in (2), $s=0$, as the point where the diameters and, therefore, the propagation constants of the adjacent microfiber segments are equal (Fig. 1), i.e.,

$$\beta_1(0) = \beta_2(0). \tag{3}$$

Existence of this point is critical for effective interfiber coupling [16], [17]. In the neighborhood of $s=0$, the electromagnetic field amplitudes $A_1(s)$ and $A_2(s)$ are related by the coupled wave equations [16]

$$\frac{\partial}{\partial s}\begin{pmatrix}A_1(s)\\A_2(s)\end{pmatrix} = i\begin{pmatrix}\Delta\beta(s) & \kappa(s)\\ \kappa(s) & -\Delta\beta(s)\end{pmatrix}\begin{pmatrix}A_1(s)\\A_2(s)\end{pmatrix}$$

$$\Delta\beta(s) = \frac{1}{2}\left(\beta_1(s)-\beta_2(s)\right) \tag{4}$$

where the coupling coefficients are expressed through the overlap integrals of the transverse modes $\mathbf{F}_1(\mathbf{r})$ and $\mathbf{F}_2(\mathbf{r})$ by (A1) given in the Appendix.

Away from the coupling region $\kappa(s)=0$ and solutions of the coupling wave equation, (4) has the form

$$A_1^{\pm}(s) = A_{01}^{\pm}\exp\left(i\int_0^{s}\Delta\beta(s)\,ds\right)$$

$$A_2^{\pm}(s) = A_{02}^{\pm}\exp\left(-i\int_0^{s}\Delta\beta(s)\,ds\right) \tag{5}$$

where the signs $+/-$ refer to the left/right hand side away from the coupling region. From (2) and (5), the condition of continuity of electromagnetic field along the microfiber loop has the form

$$A_{02}^{-} = A_{01}^{+}\exp\left(i\int_0^{S}\beta(s)\,ds\right) \tag{6}$$

where S is the length of the loop.

B. Transmission Amplitude

It can be found from the coupled wave equation (4) that the functions $A_1(s)$ and $A_2(s)$ satisfy the conservation relation $|A_1(s)|^2+|A_2(s)|^2 = \text{const}$. Therefore, the ingoing and outgoing amplitudes A_{0j}^{-} and A_{0j}^{+} in (5) are connected with the unitary matrix U as

$$\begin{pmatrix}A_{01}^{+}\\A_{02}^{+}\end{pmatrix} = U\begin{pmatrix}A_{01}^{-}\\A_{02}^{-}\end{pmatrix}$$

$$U = e^{i\phi}\begin{pmatrix}\cos(K)e^{i\theta} & \sin(K)e^{i\varphi}\\ -\sin(K)e^{-i\varphi} & \cos(K)e^{-i\theta}\end{pmatrix}. \tag{7}$$

Here, the expression for U is a general parametric representation of a 2×2 unitary matrix with real parameters ϕ, φ, θ, and K. These parameters can be determined by solving (4).

The transmission amplitude of the MLR is defined as

$$T = \frac{A_{02}^{+}}{A_{01}^{-}}. \tag{8}$$

Substituting (6) and (7) into (8), we find

$$T = e^{i(\phi-\varphi)} \frac{e^{i\Theta} - \sin(K)}{1 - \sin(K)e^{i\Theta}}$$

$$\Theta = \int_0^S \beta(s)\, ds + \phi + \varphi. \tag{9}$$

The transmission amplitude appears to be independent of θ and dependent on ϕ and φ only to a qualitatively insignificant extent. In fact, the prefactor $e^{i(\phi-\varphi)}$ in (9) does not affect the absolute value of the transmission amplitude and contributes only slightly to the delay time near resonances. Also, the phase $\phi + \varphi$ in Θ only introduces a relatively small shift to the position of transmission resonances.

The MLR is an all-pass device, and for lossless propagation, $|T| = 1$. The losses in the microfiber loop can be taken into account with a complex-valued propagation constant β, which results in a complex-valued phase Θ. If losses are uniformly distributed along the microfiber length, we still have $\mathrm{Im}(\Delta\beta) = 0$ and the imaginary component of propagation constant does not enter the coupling wave equation (4). Introducing the roundtrip attenuation γ and roundtrip phase increment Ψ

$$\Psi = \mathrm{Re}(\Theta), \quad \gamma = 2\mathrm{Im}(\Theta) \ll \Psi \tag{10}$$

and ignoring the phase prefactor, we can rewrite (9) in the form [10], [13]–[15]

$$T = \frac{e^{-\frac{\gamma}{2}} e^{i\Psi} - \sin(K)}{1 - \sin(K) e^{-\frac{\gamma}{2}} e^{i\Psi}}. \tag{11}$$

The parameter K characterizes the coupling between adjacent microfiber segments. If $K = 0$, then the loop is decoupled and, from (11), the MLR transmission behavior is similar to that of a straight microfiber. In the opposite case of strong coupling, the resonances in transmission amplitude occur only if the coupling parameter K is close to the values [10]

$$K_m = \frac{\pi}{2}(2m+1), \quad m = 1, 2, \ldots \tag{12}$$

which correspond to the full transmission of electromagnetic field from one of the adjacent fiber segments to another. Then the resonances in transmission amplitude correspond to the condition

$$\Psi = \Psi_{mn} = \pi(m + 2n) \tag{13}$$

where n is an integer.

C. Q-factor and Finesse

The performance of a resonator is indicated by its Q-factor, which can be determined as the ratio of the radiation wavelength in free space λ to the full-width at half-maximum (FWHM) of the resonance at this wavelength $\Delta\lambda$: $Q = \lambda/\Delta\lambda$. The MLR resonances are well defined only for small roundtrip attenuation $\gamma \ll 1$. Then, the Q-factor of the MLR can be defined from (11) as

$$Q = \frac{\lambda}{(K - K_m)^2 + \gamma} \int_0^S \frac{\partial\beta}{\partial\lambda}\, ds \tag{14}$$

where the propagation constant is considered as a function of wavelength [16]. The Q-factor defined by (14) is often called the loaded Q-factor. Sometimes, it is also useful to introduce the intrinsic Q-factor of a resonator, which is defined as

$$Q_{in} = \frac{\lambda}{\gamma} \int_0^S \frac{\partial\beta}{\partial\lambda}\, ds. \tag{15}$$

This Q-factor takes into account only internal losses of the MLR assuming full coupling ($K = K_m$).

The finesse of a resonator is defined as the ratio of its free spectral range (FSR) to the resonance FWHM: $F = \mathrm{FSR}/\Delta\lambda$. For well-defined resonances

$$F = \frac{2\pi}{(K - K_m)^2 + \gamma}. \tag{16}$$

In the approximation considered, the components contributing to the reduction of Q-factor and finesse can be divided into geometric and material ones. The geometrical component $(K - K_m)^2$ characterizes the deviation from the full interfiber transfer condition (12). This component is determined by the shape of the coupling microfiber segments and their mutual positions. The material component γ empirically characterizes losses in the microfiber due to microscopic elastic and inelastic scattering of light.

Currently, the propagation losses achieved for the silica microfiber with diameter $d \sim 1$ μm is $\gamma/S \sim 5 \times 10^{-3}$ mm^{-1} [3]. This is four orders of magnitude greater than the losses in silica microcavities and telecommunication single-mode fibers. Taking into account the roundtrip loss only, and estimating the integral in (14) as $\sim \beta S/\lambda$, we obtain for the maximum Q-factor

$$Q_{\max} \sim \frac{\beta S}{\gamma}. \tag{17}$$

Inserting into (17) the experimental value $\gamma/S \sim 5 \times 10^{-3}$ mm^{-1} for the silica microfiber and $\beta \sim 5$ μm^{-1}, we have $Q_{\max} \sim 10^6$. It is feasible that, by improving the microfiber drawing technique, the propagation losses can be reduced down to those achieved in fused silica microcavities and single-mode optical fibers. Accordingly, the Q-factor of an MLR has a potential of being as large as the one of the silica glass microcavities, i.e., $\sim 10^{10}$.

D. Models of Directional Couplers

Solving the coupling wave equations (4) allows us to determine the coupling parameter K in the expression for the transmission amplitude (11). In this section, we consider two models of the adjacent microfiber segments in the region of coupling.

1) The propagation constants of the adjacent microfiber segments are close, i.e., $\Delta\beta(s) \ll \kappa(s)$.
2) The propagation constants of the adjacent microfiber segments are equal at a point $s = 0$ [see Fig. 1 and (3)] and their difference linearly changes near this point growing up to the values $\Delta\beta(s) \sim \kappa(0)$. This case can be treated with the so-called Landau–Zener model.

In both of these models, the coupling parameter K can be found in an analytical form useful for estimates and understanding the MLR performance.

1) Coupling of the Microfiber Segments With Close Diameters: For microfiber segments with equal diameters $\Delta\beta(s) \equiv 0$, (4) can be solved exactly. Then

$$K = \int_{s_1}^{s_2} \kappa(s)\, ds. \tag{18}$$

The integral in (18) is taken along the coupling region $s_1 < s < s_2$. In practice, fabrication of a microfiber with high degree of uniformity is a challenging problem being addressed in several recent papers [1]–[3]. For microfiber segments with close diameters, under the condition $\Delta\beta(s) \ll \kappa(s)$, the solution of (4) can be found by perturbation theory. From [5], it can be found that near the full coupling condition $|K_0 - K_m| \ll 1$

$$K = K_m + \sqrt{(K_0 - K_m)^2 + \varepsilon^2} \tag{19}$$

$$K_0 = \int_{s_1}^{s_2} \kappa(s)\, ds, \quad \varepsilon = \int_{s_1}^{s_2} \Delta\beta(s) \sin\left(2\int_{s}^{s_2} ds'\kappa(s')\right) ds. \tag{20}$$

Equations (19) and (20) allow to estimate the reduction of the MLR Q-factor due to microfiber nonuniformity. From (19), the minimum possible deviation of the coupling parameter K from its resonance value K_m is ε. Estimating $\kappa(s_2 - s_1) \sim 1$, $\varepsilon \sim \Delta\beta/\kappa \sim \Delta d\beta/\kappa d$, and $\partial\beta/\partial\lambda \sim \beta/\lambda$, where d is the diameter of the microfiber and Δd is the diameter variation, and neglecting losses $\gamma = 0$, we have from (14)

$$Q_{\max} \sim \frac{\kappa^2 d^2 S}{(\Delta d)^2 \beta}. \tag{21}$$

Setting the coupling length $s_2 - s_1 \sim \kappa^{-1} \sim 10$ μm, the microfiber diameter $d \sim 1$ μm, the loop length $S \sim 10^3$ μm, the propagation constant $\beta \sim 5$ μm, and the relative diameter variation $\Delta d/d \sim 10^{-3}$ over 10 μm [2], we have $Q_{\max} \sim 10^6$. From this estimate, the uniformity of the microfiber is critical for achieving the high Q-factor. However, (21) significantly underestimates the Q-factor for special dependencies $\Delta\beta(s)$. For example, if the coupling region is symmetric with respect to the plane $s = 0$, then $\kappa(s)$ is a symmetric and $\Delta\beta(s)$ is an asymmetric function. At resonance, $K_0 = (\pi/2)(2m + 1)$ (12), which together with the symmetry condition gives $\varepsilon = 0$. The latter means zeroing the first order in $\Delta\beta$ correction to K in (19) and much greater Q-factors than those predicted by (21).

2) Landau–Zener Formula for Coupling Between Microfiber Segments With Smoothly Varying Diameters: Consider the case of an adiabatically smooth variation of $\Delta\beta(s)$ and $\kappa(s)$ near the zero of $\Delta\beta(s)$. Then, the transition of the electromagnetic field from one microfiber segment to another one is complete [16], [17]. In this limiting case, we simply have

$$K = \frac{\pi}{2}. \tag{22}$$

The electromagnetic field transition near the zero of $\Delta\beta(s)$ can be studied with the Landau–Zener approximation developed in quantum mechanics [19]. Assume that the coupling region is symmetric with respect to the plane $s = 0$. Then, $\Delta\beta(0) = 0$ [this is (3)], and $d\kappa/ds|_{s=0} = 0$. In the immediate neighborhood of the point $s = 0$, we can set $\beta(s) = \beta_s(0)s$ and $\kappa(s) = \kappa(0)$. Then the coupling wave equation (4) can be reduced to the parabolic cylinder differential equation. Solutions of this equation can be expressed through the functions of parabolic cylinder. As a result, the coupling parameter is determined by the Landau–Zener formula [17], [19]

$$K = \arcsin\left[\sqrt{1 - \exp\left(-\frac{\pi\kappa^2(0)}{\beta_s(0)}\right)}\right]. \tag{23}$$

From this equation, if the propagation constant is an adiabatically slow varying function so that $\beta_s(0) \ll \pi\kappa^2(0)$, then K is exponentially close to the resonant coupling parameter defined by (19). In the opposite case, if $\beta_s(0) \gg \pi\kappa^2(0)$, then K is close to zero and the microfiber segments are decoupled. Equation (20) is important for modeling the MLR. It defines the rate of microfiber nonuniformity at which one can expect the proximity of the coupling parameter to its resonance value.

III. Demonstration of the High-Q MLR

This section describes the method of fabrication of MLR in free space and demonstrates the high-Q MLR. The MLR in free space is a stand-alone device whose performance is not affected by coupling to the supporting parts. The Q-factor of this resonator depends only on the microfiber's own transmission losses and coupling efficiency.

A. Fabrication of the MLR

Fabrication of the MLR consists of drawing the microfiber and then bending it into a self-coupling loop. The method of drawing is illustrated in Fig. 2. We fabricate the biconical taper having a micrometer-order diameter waist with the CO_2 laser indirect drawing technique [6]. A standard single-mode fiber is placed into a sapphire capillary, which is heated by the radiation of a CO_2 laser and plays the role of a microfurnace. The CO_2

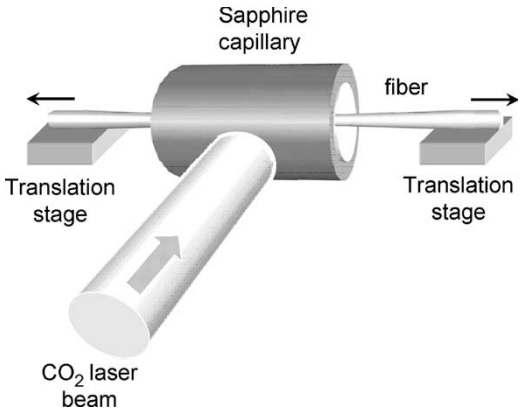

Fig. 2. Illustration of the microfiber drawing method with the CO_2 laser indirect heating technique. The optical fiber is placed into a sapphire capillary that is heated with a CO_2 laser beam. The sapphire capillary plays a role of a microfurnace inside which the fiber is drawn down to micrometer-order diameter with translation stages.

laser drawing technique may have certain advantages compared to the conventional microfiber drawing in a flame [2], [3] or in close proximity to a flame [1] due to its cleanness and strong suppression of convection currents near the microfiber. The latter allows the fabrication of very thin microfibers having diameters below 100 nm [6]. The characteristic diameter of a microfiber used for fabrication of an MLR is around 1 μm. An example of the microfiber diameter variation measured with a scanning electron microscope (SEM), which was used in our first demonstration of the sub-micrometer diameter MLR, is given in [7]. The minimum microfiber diameter, which was approximately uniform along 1 mm of its length, was $\sim$ 0.66 μm. In the experiments of the present paper, the minimum microfiber diameter was larger (~ 0.9 μm), and its variation in the coupling region was smoother than in [7], which resulted in smaller microfiber losses, higher coupling efficiency, and, eventually, higher Q-factor of the fabricated MLR.

The setup for MLR fabrication is illustrated in Fig. 3. It consists of three translation stages, which can move the microfiber ends with respect to each other in three directions, and a rotation stage, which can twist the microfiber. The total length of the drawn taper was 25 mm. It had a uniform waist of around 2-mm length with $\sim$ 0.9-μm diameter. The microfiber loop was created by manipulating the translation stages and rotation stage. Controlling the shape of the microfiber with the stages and an optical microscope, we coiled the taper waist into a self-touching loop. Fig. 4 shows an optical microscope image of the loop with the input and output ends aligned parallel to each other. Parallel alignment was possible due to surface attraction forces (Van der Waals and electrostatic), which kept the ends together, apparently overcoming the elastic forces that would tend to straighten out the microfiber.

B. MLR Transmission Characteristics

The spectrum of the unpolarized light transmitted through the MLR was measured with an optical spectrum analyzer (OSA) in the C-band from 1520 to 1570 nm. Fig. 5 shows dramatically uniform and smooth transmission spectra, which were

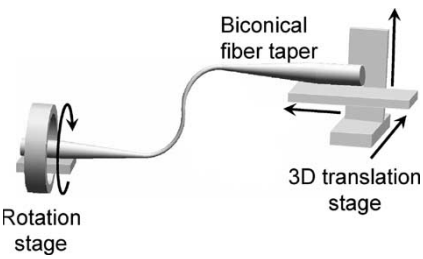

Fig. 3. Illustration of the microfiber bending and looping in free space using 3-D translation stage and rotation stage.

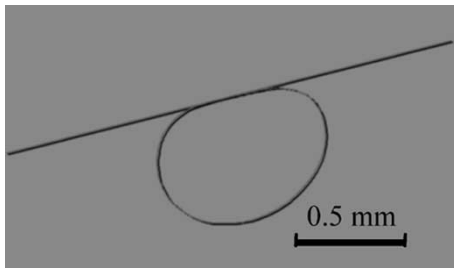

Fig. 4. Optical microscope image of an MLR.

obtained by tuning the loop ends to different mutual positions by translation of the taper ends with respect to each other. In our analysis of experimental data, we neglected coupling between TE and TM polarization states and expressed the total power transmitted through the MLR W as a sum of partial transmission powers for TE and TM polarizations, i.e.,

$$W = |T_1|^2 + |T_2|^2 \tag{24}$$

where each of the transmission amplitudes T_1 and T_2 corresponds to one of the polarization states TM or TE. The transmission amplitudes T_j in (24) are expressed through the polarization-dependent parameters γ_j and K_j by (11). We fitted the experimental spectra with (11) and (24) averaged over the interval of instrumental averaging equal to 0.01 nm for the OSA we used. The results shown in Fig. 5(a) and (b) were obtained by tuning the MLR shown in Fig. 4, while the result of Fig. 5(c) was obtained with another MLR comprised of a microfiber fabricated with the same drawing parameters. We found that the loaded/intrinsic Q-factor and the finesse of the resonances in Fig. 5(a) achieve the values of 22 000/60 000 and 9, in Fig. 5(b), these values are 95 000/630 000 and 42, and in Fig. 5(c), these values are 120 000/155 000 and 35, respectively. The achieved loaded Q-factor is close to the largest Q-factors recently demonstrated for planar ring resonators [20]–[23]. The small asymmetry in each of the resonances in Fig. 5(a) is due to the superposition of TE and TM modes, which are shifted in phase and have different loaded Q-factors. In Fig. 5(b) and (c), the resonances of TE and TM polarization states are well separated and their amplitudes are slowly changing with wavelength. The change is caused by the weak dependence of coupling coefficient and attenuation on wavelength. For the case of Fig. 5(c), an example of fitting the theoretical model to the experimental resonance peak is shown in Fig. 6. The best fit is achieved with the following parameters: $\gamma_1 = 0.14$,

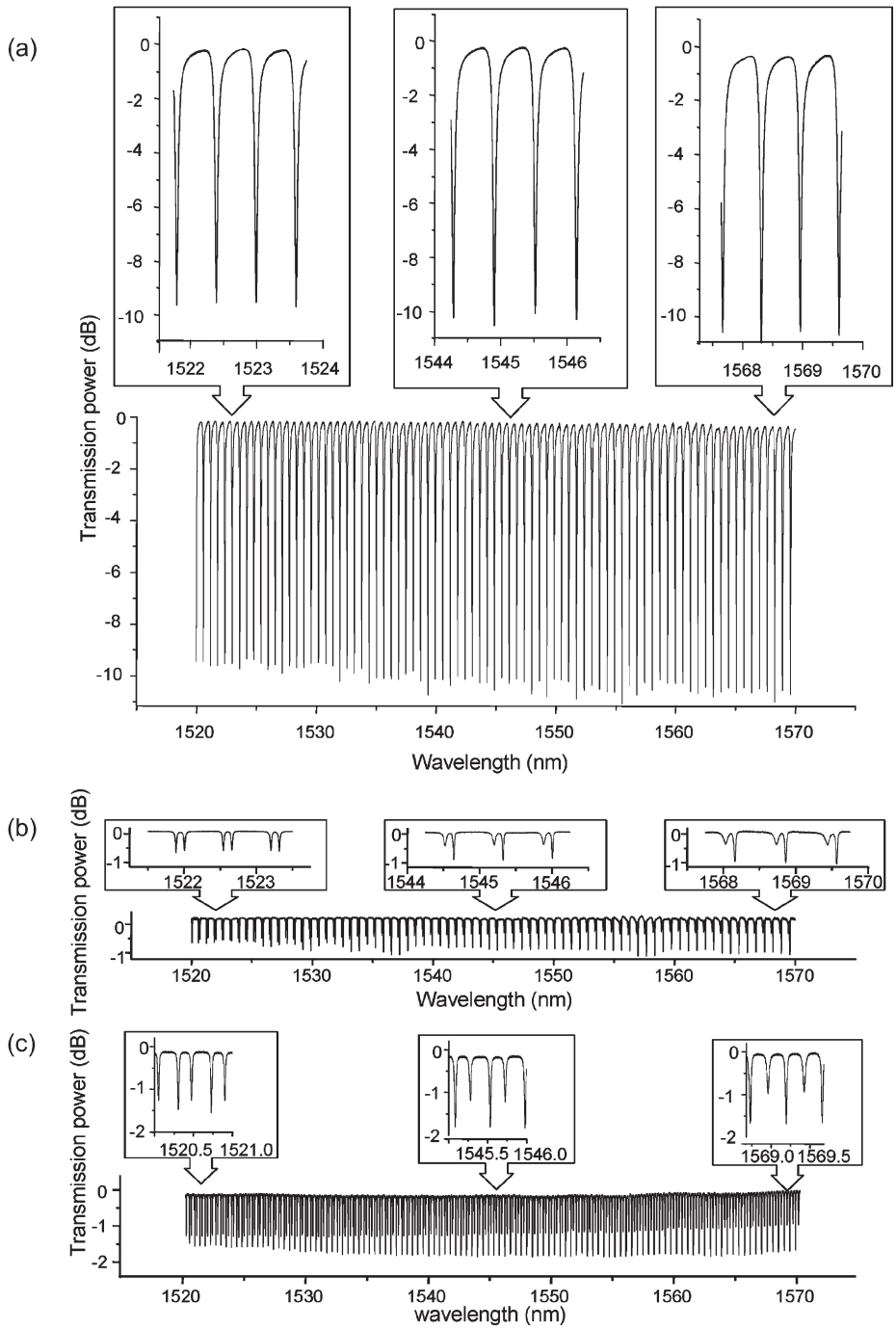

Fig. 5. Transmission spectra of MCR tuned to loaded Q-factor of (a) 22 000, (b) 98 000, and (c) 120 000.

$\gamma_2 = 0.19$, $\sin(K_1) = 0.981$, and $\sin(K_2) = 0.985$. It is interesting to estimate the coupling parameter of the MLR using the theory of Section II. From the image of the MLR shown in Fig. 4, the width of the coupling region is $\sim 10 - 100$ μm; therefore, the coupling coefficient $\kappa \sim 10^{-1} - 10^{-2}$ μm^{-1}. Let us estimate $\beta \sim 5$ μm^{-1} and the characteristic length of variation of propagation constant $s_c \sim 10^3$ μm. Then, we find that, depending on specific values of κ, β, and s_c within the indicated range, the coupling parameter defined by (23) can be away from the resonance value as well as exponentially close to it. If the microfiber diameter variation is known (e.g., from the SEM measurement), the accurate values for the parameters entering (23) can be calculated numerically. The numerical solution, which is beyond the scope of this paper, would allow better understanding of the mechanism of microfiber coupling following from our experimental data.

IV. MLR as an Ultrafast Direct Contact Temperature Sensor

Microring and microdisk resonators have been suggested as sensors of physical, chemical, and biological changes of the

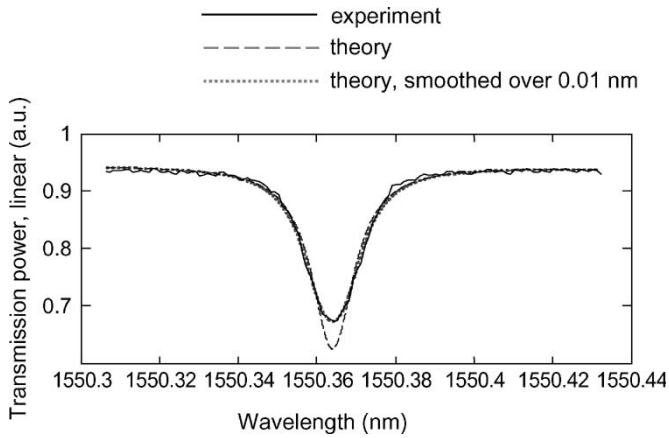

Fig. 6. Fitting the experimental data of Fig. 5(c) near a resonance (solid) with the theoretical calculation (dashed) averaged over the interval of instrumental averaging equal to 0.01 nm (dotted).

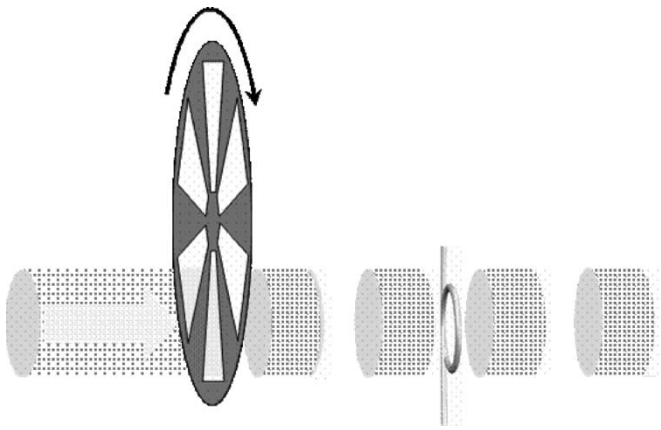

Fig. 7. Periodic ON/OFF heating of an MLR using a CO_2 laser beam and a beam chopper.

environment [24]–[26]. In fact, the positions of the narrow transmission resonances are very sensitive to variations in the effective refractive index and length of the microring, which in turn are affected by the refractive index of the ambient medium as well as by temperature, pressure, and applied radiation.

A MLR positioned in free space has a much larger interfacial contact area with the environment than a microring resonator mounted on a substrate. Therefore, the MLR should serve as a more sensitive detector of environmental changes. In particular, this ultrathin and ultralight device can perform as an ambient gas local temperature sensor. In the Section IV-A, we consider the theory of periodic heating of a microfiber. In Section IV-B, we experimentally demonstrate an MLR subjected to periodic heating by a CO_2 laser beam.

A. Theory of the Microfiber Heating and Cooling

Heating and cooling of a fiber can be described by the lumped system equation [27], [28]

$$\frac{dT(t)}{dt} = -\frac{1}{\tau}\left(T(t) - T_a\right) + \Xi(t)$$
$$\tau = \frac{c_p \rho V_f}{A_f h}, \quad \Xi(t) = \frac{q(t)}{c_p \rho} \tag{25}$$

where $T(t)$ is the temperature of the microfiber as a function of time t, T_a is the temperature of the ambient air, A_f is the surface of the fiber, V_f is the volume of the fiber, ρ is the density of the fiber material, c_p is its the specific heat, h is the convection coefficient, and $q(t)$ is the heat generation rate per unit volume, which, in our case, is caused by laser heating. The first term in the right-hand part of (1) describes fiber cooling due to convection and the second term describes fiber heating by the laser beam.

For the cylindrical microfiber with radius r, $V_f/A_f = (\pi r^2)/(2\pi r) = r/2$, and we have for the relaxation time

$$\tau = \frac{c_p \rho r}{2h}. \tag{26}$$

Assuming that the microfiber has not been heated initially $(T(0) = T_a)$, we find the solution of (25) in the form

$$T(t) = T_a + \int_0^t dt' \Xi(t') \exp\left(\frac{t' - t}{\tau}\right). \tag{27}$$

For $\Xi(t) = \text{const}$, the equilibrium temperature is defined from (25) by setting the time derivative dT/dt equal to zero.

In our experiment, the microfiber is heated periodically by turning the power of the incident laser beam ON and OFF using the beam chopper, as illustrated in Fig. 7. Then, the temperature of the fiber is determined by (25), where

$$\Xi(t) = \frac{\Xi_0}{2} \sum_{n=0}^{\infty} \left[\theta(t - nt_0)\theta\left(\left(n + \frac{1}{2}\right)t_0 - t\right)\right]$$
$$\Xi_0 = \frac{kP}{A_b r c_p \rho} \tag{28}$$

where P is the laser power, A_b is the cross-section of the laser beam, $k < 1$ is the power absorption rate, t_0 is the period of ON/OFF switching, and $\theta(x)$ is the Heaviside function [$\theta(x) = 1$ for $x > 0$ and $\theta(x) = 0$ for $x \leq 0$].

It is seen from (27) and (28) that the characteristic relaxation time, both in the case of heating and cooling, does not depend on the heating power and is equal to the relaxation time τ defined by (26). For the silica microfibers considered in this paper, we use the following values of parameters: $h \approx 400\ \text{W}/(\text{m}^2\text{K})$ [28], $c_p = 837\ \text{J}/(\text{kg} \cdot \text{K})$, $\rho = 2200\ \text{kg/m}^3$, $r = 0.5\ \mu\text{m}$, $P = 10\ \text{W}$, $A_b = 10$, and $k = 0.1\ \text{mm}^2$, which yields the relaxation time

$$\tau = 0.002\ \text{s}. \tag{29}$$

For a regular optical fiber having a diameter 100 times greater, the relaxation time is, proportionally, 0.2 s.

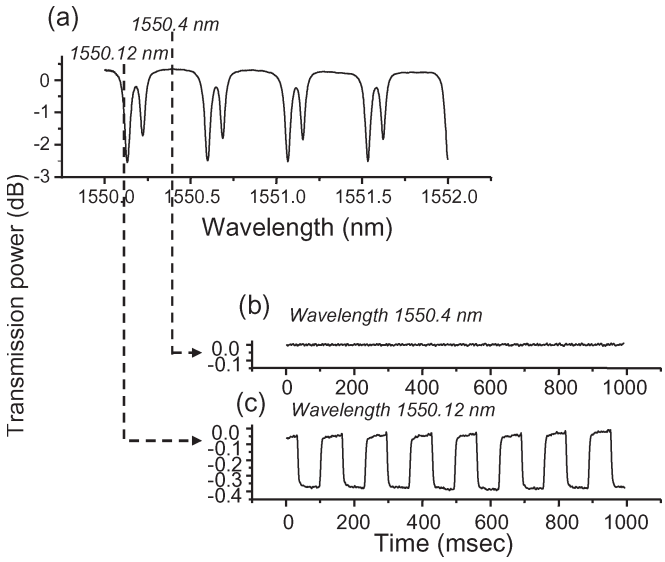

Fig. 8. (a) Transmission spectrum of MLR used as a temperature sensor. Transient behavior of MLR periodically heated by CO_2 laser at wavelength of (b) 1550.4 nm (flat spectrum) and (c) 1550.12 nm (steep spectrum).

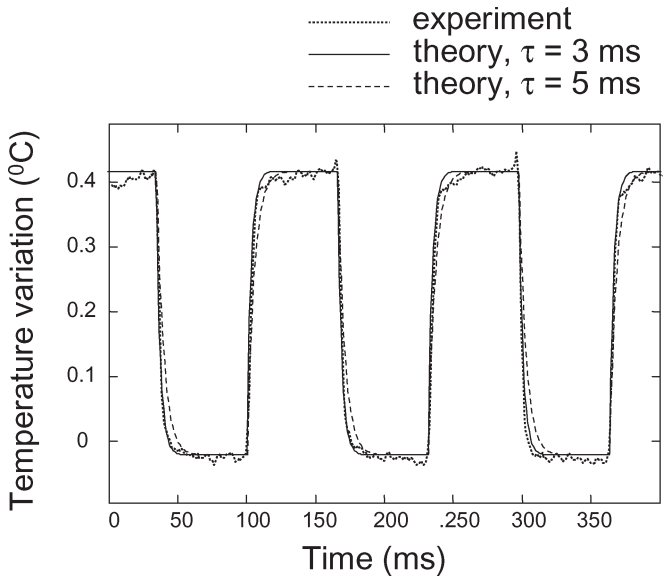

Fig. 9. Comparison of the rescaled oscillations of the linear transmission of the microloop and the temperature variation calculated from (27) and (28). It is seen that the theoretical curve with $\tau = 0.003$ s provides better fit than the curve with $\tau = 0.005$ s.

B. Fast MLR Response to the Temperature Variation: Experiment

In order to model the MLR temporal response, we placed an MLR, whose transmission spectrum is shown in Fig. 8(a), into a 7.5-Hz frequency ON/OFF-modulated CO_2 laser field. First, the OSA was tuned to 1550.4 nm and we recorded the time dependence of transmitted power corresponding to a flat region of the spectrum in Fig. 8(a). The result shown in Fig. 8(b) indicates no visible time response. However, at 1550.12 nm, which corresponds to a steep region near resonance, we observed the oscillations of transmission power shown in Fig. 8(c). Fig. 9 compares the results of fitting the experimental data of Fig. 8(c) with theoretical dependencies calculated from (27) and (28) for relaxation times $\tau = 3$ μs and 5 μs. From this figure, the experimental measured relaxation time is $\tau = 3$ μs, in good agreement with the theoretical value 2 μs obtained from (29). From the transient oscillations in Fig. 8(c), we could calculate the magnitude of temperature variation, i.e., 0.4 K. The full measured temperature scale, which is ~ 1 K in our experiment, can be increased by orders of magnitude with decreasing Q and/or choosing a less steep spectral region. The temperature resolution of the demonstrated MLR thermometer is determined by the resolution of the optical power measurement device used (typically $\sim 10^{-4}$ of full scale [18]). Thus, in the case considered here, the temperature resolution can be as small as ~ 0.1 mK.

V. Discussion and Summary

We reported the experimental demonstration of a high-Q all-in-one-fiber MLR whose Q-factor competes with the largest Q-factors achieved for in-plane microring resonators fabricated lithographically. The MLR resonances have very smooth and similar behavior in the full C-band. We believe that the Q-factor demonstrated in this paper can be significantly enhanced by optimizing our simple microfiber fabrication process. The fact that the MLR was created in free space as a stand-alone device has the advantage that the MLR's performance is not affected by the properties of a supporting substrate. It is feasible that placing an MLR on a flat substrate with a lower index or wrapping it around a cylinder will not reduce its Q-factor significantly. In fact, low loss silica microfibers, which were placed on an aerogel substrate and had their internal bending stresses relaxed by annealing, have been recently demonstrated [19]. Another interesting possibility for the microfiber-based photonics is the use of microfibers fabricated from a higher index glass placed on a regular silica glass substrate. We believe that the current demonstration of MLR can be extended to a more complex multiturn MCR, providing a novel type of very compact and low-loss broadband filtering and group delay devices for optical communications as well as for local sensing of physical, chemical, and biological parameters of the environment.

Appendix
Expression for the Coupling Coefficient

Expression for the coupling coefficient in the couplingwave equations (4) has the form [5], [16], shown in (A1) at the top of the next page, and the transverse modes $\mathbf{F}_j(\mathbf{r})$ are assumed normalized

$$\int\limits_{x^2+y^2<\infty} dxdy\,(F_{0x}(\mathbf{r})F_{0x}(\mathbf{r}) + F_{0y}(\mathbf{r})F_{0y}(\mathbf{r})) = 1. \quad \text{(A2)}$$

In (A1), n_f and n_e are the fiber and external refractive indices, respectively, and the last integral is taken along the circle at the surface of the fiber. Equations (A1) and (A2) are written in the local orthogonal coordinate system along the microfiber $\mathbf{r} = (x, y, s)$, where y is normal to s and lies in the plane of Fig. 1 and x is normal to y and s.

$$\kappa(s) = \frac{\left(n_f^2 - n_e^2\right)}{\beta} \times \left\{ \frac{2\pi^2}{\lambda^2} \iint\limits_{x^2+y^2<R^2(s)} dxdy \left[F_{1x}(\mathbf{r})F_{2x}(\mathbf{r}) + F_{1y}(\mathbf{r})F_{2y}(\mathbf{r})\right] + \frac{1}{2n_f^2} \oint\limits_{x^2+y^2=R^2(s)} \frac{dl}{r} \left[(xF_{1x}(\mathbf{r}) + yF_{1y}(\mathbf{r})) \times \left(\frac{\partial F_{2x}(\mathbf{r})}{\partial x} + \frac{\partial F_{2y}(\mathbf{r})}{\partial y}\right)\right] \right\} \quad \text{(A1)}$$

REFERENCES

[1] L. Tong, R. R. Gattass, J. B. Ashcom, S. He, J. Lou, M. Shen, I. Maxwell, and E. Mazur, "Subwavelength-diameter silica wires for low-loss optical wave guiding," *Nature*, vol. 426, no. 6968, pp. 816–819, Dec. 2003.

[2] G. Brambilla, V. Finazzi, and D. J. Richardson, "Ultra-low-loss optical fiber nanotapers," *Opt. Express*, vol. 12, no. 10, pp. 2258–2263, May 2004.

[3] S. G. Leon-Saval, T. A. Birks, W. J. Wadsworth, and P. S. J. Russell, "Guidance properties of low-contrast photonic bandgap fibres," *Opt. Express*, vol. 12, no. 13, pp. 2864–2869, Jun. 2004.

[4] K. J. Vahala, "Optical microcavities," *Nature*, vol. 424, no. 6950, pp. 839–846, Aug. 2003.

[5] M. Sumetsky, "Optical fiber microcoil resonator," *Opt. Express*, vol. 12, no. 10, pp. 2303–2316, May 2004.

[6] M. Sumetsky, Y. Dulashko, and A. Hale, "Fabrication and study of bent and coiled free silica nanowires: Self-coupling microloop optical interferometer," *Opt. Express*, vol. 12, no. 15, pp. 3521–3531, Jul. 2004.

[7] M. Sumetsky, Y. Dulashko, J. M. Fini, and A. Hale, "Optical microfiber loop resonator," *Appl. Phys. Lett.*, vol. 86, Apr. 2005. paper 161108.

[8] B. E. Little, "A VLSI photonics platform," in *Proc. Optical Fiber Communication Conf. (OFC)*, Atlanta, GA, 2003, pp. 444–445.

[9] M. Sumetsky, "Uniform coil optical resonator and waveguide: Transmission spectrum, eigenmodes, and dispersion relation," *Opt. Express*, vol. 13, no. 11, pp. 4331–4340, May 2005.

[10] L. F. Stokes, M. Chodorow, and H. J. Shaw, "All-single-mode fiber resonator," *Opt. Lett.*, vol. 7, no. 6, pp. 230–288, Jun. 1982.

[11] C. Caspar and E.-J. Bachus, "Fibre-optics micro-ring-resonator with 2 mm diameter," *Electron. Lett.*, vol. 25, no. 11, pp. 1506–1508, Oct. 1989.

[12] M. Sumetsky, Y. Dulashko, J. M. Fini, A. Hale, and D. J. DiGiovanni, "Demonstration of a microfiber loop optical resonator," presented at the Optical Fiber Communication Conf., Anaheim, CA, 2005, Postdeadline Paper PDP10.

[13] C. K. Madsen and G. Lenz, "Optical all-pass filters for phase response design with applications for dispersion compensation," *IEEE Photon. Technol. Lett.*, vol. 10, no. 7, pp. 994–996, Jul. 1998.

[14] G. T. Paloczi, Y. Huang, and A. Yariv, "Free-standing all-polymer microring resonator optical filter," *Electron. Lett.*, vol. 39, no. 23, pp. 1650–1651, Nov. 2003.

[15] O. Schwelb, "Transmission, group delay, and dispersion in single-ring optical resonators and add/drop filters—A tutorial overview," *J. Lightw. Technol.*, vol. 22, no. 5, pp. 1380–1394, May 2004.

[16] A. W. Snyder and J. D. Love, *Optical Waveguide Theory*. London, U.K.: Chapman & Hall, 1983.

[17] R. B. Smith, "Analytic solution for linearly tapered directional couplers," *J. Opt. Soc. Amer.*, vol. 66, no. 9, pp. 882–892, Sep. 1976.

[18] K. Morishita and T. Yamaguchi, "Wavelength tunability and polarization characteristics of twisted polarization beamsplitting single-mode fiber couplers," *J. Lightw. Technol.*, vol. 19, no. 5, pp. 732–738, May 2001.

[19] L. D. Landau and E. M. Lifshitz, *Quantum Mechanics*. New York: Pergamon, 1977.

[20] C. K. Madsen, S. Chandrasekhar, E. J. Laskowski, M. A. Cappuzzo, J. Bailey, E. Chen, L. T. Gomez, A. Griffin, R. Long, M. Rasras, A. Wong-Foy, L. W. Stulz, J. Weld, and Y. Low, "An integrated tunable chromatic dispersion compensator for 40 Gb/s NRZ and CSRZ," in *Proc. Optical Fiber Communication Conf.*, Anaheim, CA, 2002, pp. FD9-1–FD9-3.

[21] G. Bourdon, G. Alibert, A. Beguin, B. Bellman, and E. Guiot, "Ultra-low loss ring resonators using 3.5% index-contrast Ge-doped silica waveguides," *IEEE Photon. Technol. Lett.*, vol. 15, no. 5, pp. 709–711, May 2003.

[22] B. E. Little, S. T. Chu, P. P. Absil, J. V. Hryniewicz, F. G. Johnson, F. Seiferth, D. Gill, V. Van, O. King, and M. Trakalo, "Very high-order microring resonator filters for WDM applications," *IEEE Photon. Technol. Lett.*, vol. 16, no. 10, pp. 2263–2265, Oct. 2004.

[23] J. Niehusmann, A. Vörckel, P. H. Bolivar, T. Wahlbrink, W. Henschel, and H. Kurz, "Ultrahigh-quality-factor silicon-on-insulator microring resonator," *Opt. Lett.*, vol. 29, no. 24, pp. 2861–2863, Dec. 2004.

[24] B. E. Little, T. Chu, and H. A. Haus, "Second-order filtering and sensing with partially coupled traveling waves in a single resonator," *Opt. Lett.*, vol. 23, no. 20, pp. 1570–1572, Oct. 1998.

[25] E. Krioukov, D. J. W. Klunder, A. Driessen, J. Greve, and C. Otto, "Integrated optical microcavities for enhanced evanescent-wave spectroscopy," *Opt. Lett.*, vol. 27, no. 17, pp. 1504–1506, Sep. 2002.

[26] S. Ashkenazi, C.-Y. Chao, L. J. Guo, and M. O'Donnell, "Ultrasound detection using polymer microring optical resonator," *Appl. Phys. Lett.*, vol. 85, no. 22, pp. 5418–5420, Nov. 2004.

[27] J. P. Holman, *Heat Transfer*. New York: McGraw-Hill, 1981.

[28] A. J. C. Grellier, N. K. Zayer, and C. N. Pannel, "Heat transfer modeling in CO_2 laser processing of optical fibres," *Opt. Commun.*, vol. 152, no. 4–6, pp. 324–328, Jul. 1998.

[29] A. Wang, H. Xiao, J. Wang, Z. Wang, W. Zhao, and R. G. May, "Self-calibrated interferometric—Intensity-based optical fiber sensors," *J. Lightw. Technol.*, vol. 19, no. 10, pp. 1495–1501, Oct. 2001.

[30] L. Tong, J. Lou, R. R. Gattass, S. He, X. Chen, L. Liu, and E. Mazur, "Assembly of silica nanowires on silica aerogels for microphotonic devices," *Nano Lett.*, vol. 5, no. 2, pp. 259–262, Feb. 2005.

M. Sumetsky, photograph and biography not available at the time of publication.

Y. Dulashko, photograph and biography not available at the time of publication.

J. M. Fini, photograph and biography not available at the time of publication.

A. Hale, photograph and biography not available at the time of publication.

D. J. DiGiovanni, photograph and biography not available at the time of publication.